Complete Link Budgets for Backscatter-Radio and RFID Systems

Joshua D. Griffin and Gregory D. Durgin

Georgia Institute of Technology
777 Atlantic Ave., Atlanta, GA 30332-0250 USA
Tel: +1 (404) 894-2951; Fax: +1 (404) 894-5935; E-mail: jdgriffin@ieee.org; durgin@ece.gatech.edu

Abstract

Backscatter radio – wireless communication by modulating signals scattered from a transponder (RF tag) – is fundamentally different from conventional radio because it involves two distinct links: the power-up link for powering passive RF tags, and the backscatter link for describing backscatter communication. Because of severe power constraints on the RF tag, a thorough knowledge of the backscatter channel is necessary to maximize backscatter-radio and radio-frequency identification (RFID) system performance. This article presents four link budgets that account for the major propagation mechanisms of the backscatter channel, along with a detailed discussion of each. Use of the link budgets is demonstrated by a practical UHF RFID portal example. The benefits of future 5.8 GHz multi-antenna backscatter-radio systems are shown. An intuitive analogy for understanding the antenna polarization of RF tag systems is presented.

Keywords: Radio frequency identification; RFID; backscatter radio; link budgets; radio propagation; scattering; back propagation; transponders; radar cross sections; diversity methods; polarization

1. Introduction

In recent years, reductions in the manufacturing costs of high-frequency integrated circuits have sparked explosive growth and research interest in backscatter-radio systems, of which the most well-known application is radio-frequency identification (RFID) for industrial supply chains. Of course, supply-chain management is only one of the many uses of backscatter radio-frequency (RF) tags. Other uses include medical telemetry, low-cost sensors, remote switches, position location and tracking devices, and passive data exchange, to name just a few. It is easy to get swept away dreaming up all of the possible uses of low-cost, low- or no-power radio tags: contact-less memory sticks, subcutaneous glucose sensors for diabetics, environmental tracking of food items, the famous "instant wireless checkout" of tagged items at the grocery store, and so on. However, whether or not any of these applications are even possible depends on the multi-faceted physics of the RF tag's radio link budget, which is the subject of this article.

In radio communications, the most critical obstacle is always received power. No signal-processing or clever power-supply scheme can overcome a radio channel that does not maintain the Shannon minimum power level for a given rate of data exchange. RF tags are further limited by the need, in passive systems, to power up their *radio frequency integrated circuits* (RFICs) through rectification of the incoming signal. Therefore, accurate calculation of the backscattered power (for information exchange) and of the forward received power (for energizing a tag's radio-frequency integrated circuit) will demonstrate the feasibility of a new application more quickly and less expensively than speculative prototyping.

After a brief survey of the state-of-the-art in backscatter RF tag technology, we present an overview of several practical RF tag link budgets. With the fundamentals in hand, we then discuss the individual physical mechanisms that influence the link budget. The emphasis is not just on accurate equations, but on illuminating the phenomena that alter the link budgets. Only an intimate understanding of these phenomena will free the engineer from merely *describing* the link to instead allowing for *design* and *innovation*. We conclude with two illustrative examples of link-budget calculations at 915 MHz and at 5790 MHz, and a discussion of a similarity between optical polarizers and antenna polarization in backscatter systems.

2. Why Backscatter Radio is Different

Radio communication becomes technologically challenging whenever special power demands are placed on at least one of the communicating nodes. For example, satellite radio is challenging because the satellite has been stranded in outer space, where power (and maintenance) are in short supply. Personal cellular radio is challenging largely because the base stations are forced to exchange information with low-cost commercial handsets that use small, stingy batteries. Passive RFID and backscatter radio are challenging because one of the communicating devices has *no* power available for communication, outside of what is received from a far-field reading device.

The goal of backscatter radio is to retrieve information from an RF tag by illuminating the device with UHF or microwave

 ISSN 1045-9243/2009/$25 ©2009 IEEE

power, and decoding modulated signals scattered back from the RF tag to the receiving antenna. The RF tag is usually so simple that it has no conventional RF receiver components: no mixers, no amplifiers, and nominal filtering. The tag serves only as a passive transponder that returns a portion of its received power with modulation. There are several ways to accomplish this. One is using a high-frequency diode (or equivalent component) at the terminals of the antenna. Shown in Figure 1, a diode current-voltage characteristic has an ac-equivalent resistance that depends on its dc bias point. With a positive dc bias voltage, the diode behaves as an RF short circuit; with a negative dc bias voltage, the diode approximates an RF open circuit. At the terminals of an antenna, this results in a reflection-coefficient change that is detectable by a far-field receiving antenna. Other types of nonlinear semiconductor devices – Schottky diodes, varactor diodes, PIN diodes, and MOSFETs – have all been used in a similar manner.

Another way in which passive RFID and backscatter radio differ from conventional radio is that the link budget for backscattered signals resembles the radar equation. This is because the RF tag's antenna is absorbing and re-emitting radio waves as a function of its load mismatch. However, the conventional one-way link budget for power received by the RF tag is also important in backscatter radio, particularly if the RF tag is purely passive. These passive tags must rectify the incoming RF waveform, and convert it to dc power for the tag's radio-frequency integrated circuit.

One simple method for converting the RF power to dc power is with a *charge pump*, constructed using the rectifier circuit shown in Figure 2a. By adding a capacitor and diode, it can be made into a full-wave rectifier or *voltage doubler*, shown in Figure 2b. This can then be cascaded to make a generic 2*N*-fold voltage multiplier, shown in Figure 2d, derived from a Dickson charge pump [2]. Voltage multipliers are important for boosting the rectified dc voltage, as a simple rectifier will only activate other components in the radio-frequency integrated circuit when the RF tag is very close to the reader. The range of the RF tag can be extended by careful optimization of the charge pump, and by conjugately matching the charge pump's impedance to that of the tag's antenna [3]. However, since even the best charge pumps become less and less efficient as V_{AC} drops below the diode turn-on voltage, there is a minimum received power required for a tag's radio-frequency integrated circuit to power up. In general, this minimum power is in the range of 50 to 500 μW for a conventional silicon radio-frequency integrated circuit, operating in the 902-928 MHZ frequency band [4]. Two notable exceptions to this rule are radio-frequency integrated circuits that consume only 16.7 μW at 869 MHz [5] and 2.7 μW at 2.45 GHz [6], using 0.5 μm two-poly, two-metal digital CMOS and 0.5 μm silicon-on-sapphire technologies, respectively. Therefore, it is apparent that the power requirements of tag radio-frequency integrated circuits will decrease as innovative designs are developed and IC technologies with low parasitics are used.

3. The Four Link Budgets of Backscatter Radio

There are essentially four types of link budgets used in backscatter radio, depending upon whether power-up issues or the flow of backscattered information is being studied.

3.1 The Power-Up Link Budget

The power-up link budget describes one-way power flow from the transmitter portion of the reader to the RF tag. Specifically, the power, P_t, is the amount of RF power coupled into the tag's radio-frequency integrated circuit, discounting any loss factors internal to the chip. This received tag power is given by the following linear-scale link budget:

$$P_t = \frac{P_T G_T G_t \lambda^2 X \tau}{(4\pi r)^2 \Theta B F}, \quad (1)$$

where P_t is the power coupled into the radio-frequency integrated circuit [W], P_T is the power transmitted by the reader [W], G_T is the load-matched, free-space gain of the transmitter antenna, G_t is the load-matched, free-space gain of the tag antenna, λ is the carrier-frequency wavelength [m], X is the polarization mismatch, τ

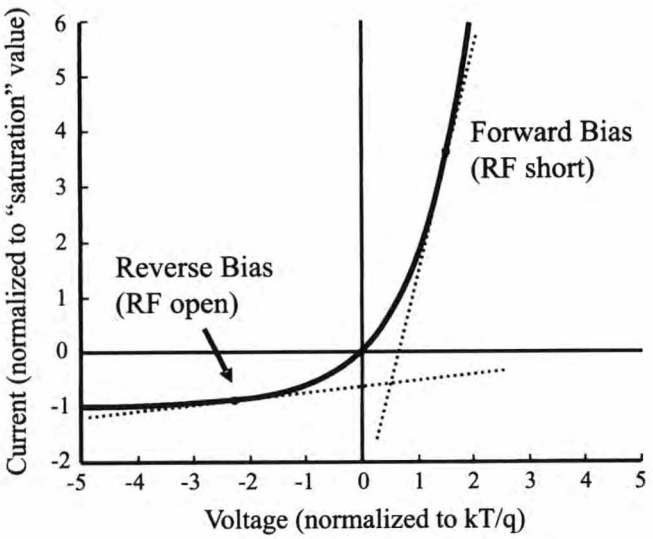

Figure 1a. A diode current-voltage (*I-V*) curve shows how a diode can be used to change the RF impedance at the terminals of an antenna.

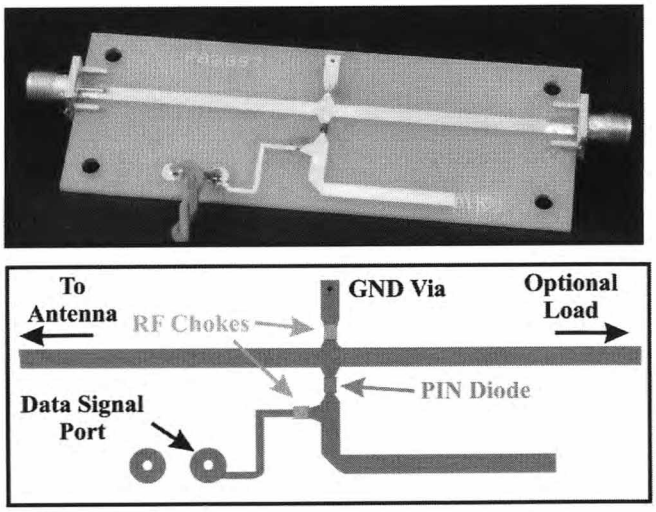

Figure 1b. A PIN diode modulator, constructed to emulate backscatter modulation at the terminals of an antenna [1].

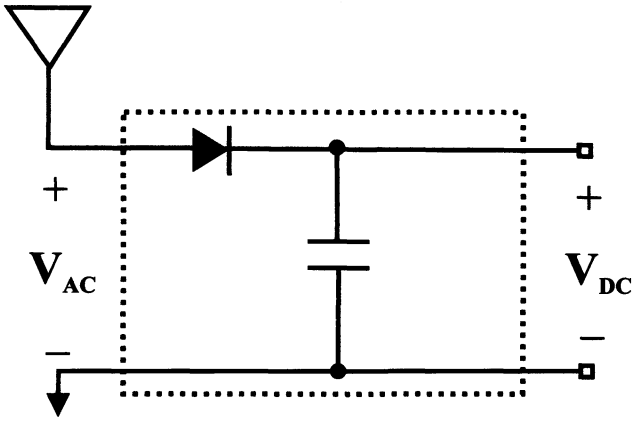

Figure 2a. A summary of different charge-pump circuits: a basic rectifier.

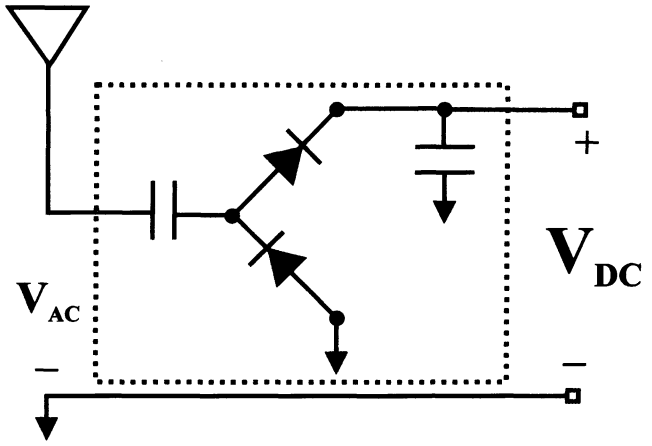

Figure 2b. A summary of different charge-pump circuits: a voltage doubler.

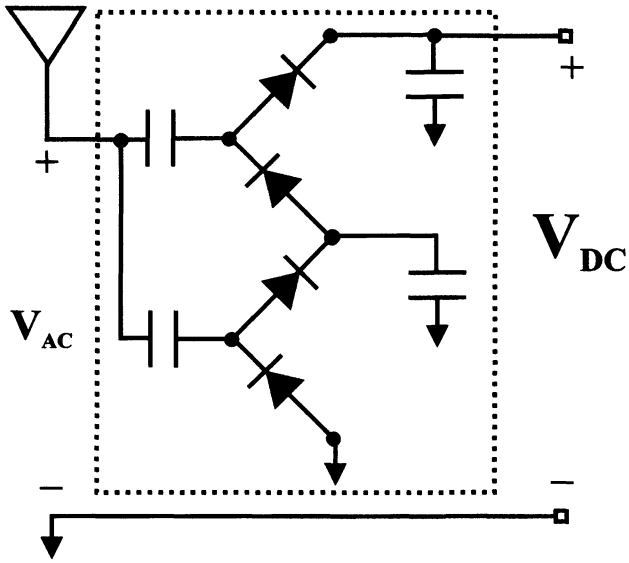

Figure 2c. A summary of different charge-pump circuits: a voltage quadrupler.

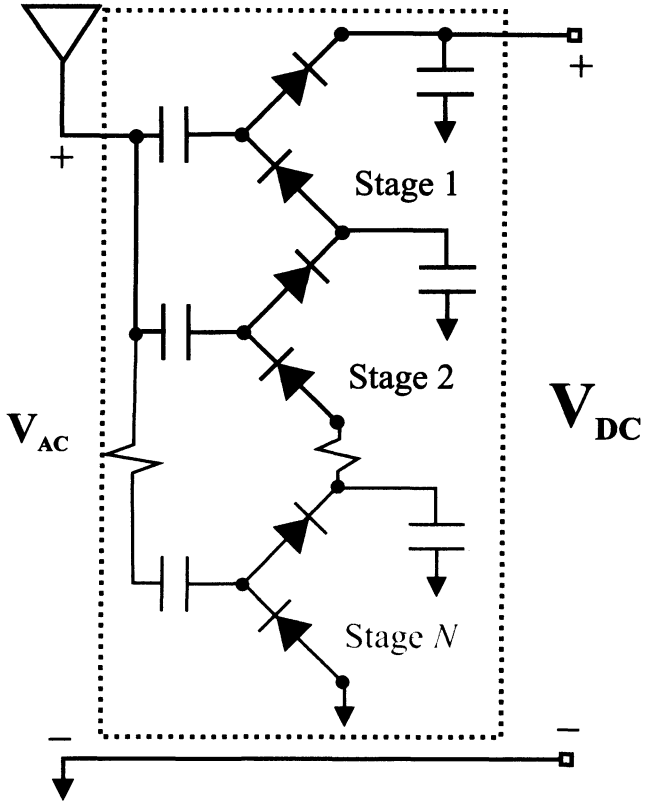

Figure 2d. A summary of different charge-pump circuits: a $2N$-fold voltage multiplier.

is the power-transmission coefficient, r is the reader-to-tag separation distance [m], Θ is the RF tag antenna's on-object gain penalty, B is the path-blockage loss, and F is the one-way power-up fade margin. Much like a conventional radio-link budget, Equation (1) depends on the separation distance, r, the antenna gains, G_T and G_t, and the transmitted power, P_T. Additionally, the unitless loss terms, B, τ, Θ, F, and X that appear in Equation (1) are described in Section 4.

3.2 The Monostatic Backscatter Link Budget

After powering-up, a sufficient amount of power must be scattered back from the RF tag to the reader for the transfer of information. There are three types of backscatter links for information exchange, each having a distinct form, as summarized in Figure 3. The first type is the *monostatic backscatter link*, where a single antenna is used at the reader for both transmission and reception. The reader's received modulated backscatter power, P_R, is given by the following linear-scale link budget:

$$P_R = \frac{P_T G_{TR}^2 G_t^2 \lambda^4 X^2 M}{(4\pi r)^4 \Theta^2 B^2 F_2}, \qquad (2)$$

where P_R is the modulated backscatter power received at the reader [W], M is the modulation factor, G_{TR} is the load-matched, free-space gain of the reader transmitter/receiver antenna, and F_2

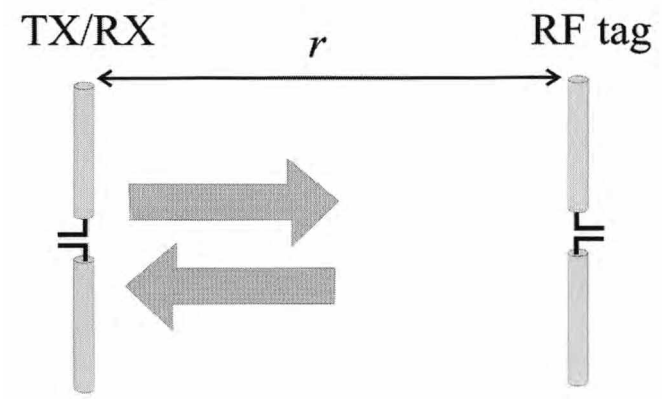

Figure 3a. The monostatic configuration, one of the three main antenna configurations in the backscatter link.

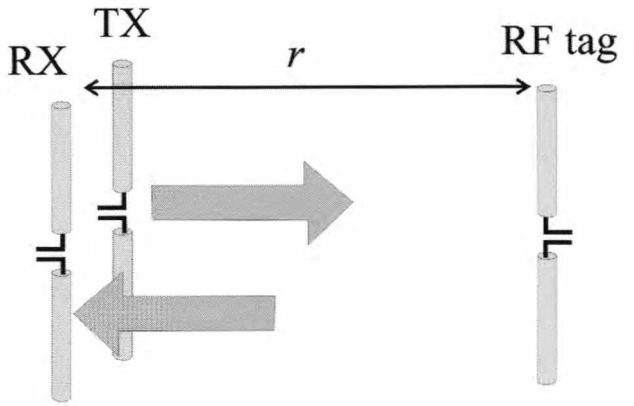

Figure 3b. The bistatic collocated configuration, one of the three main antenna configurations in the backscatter link.

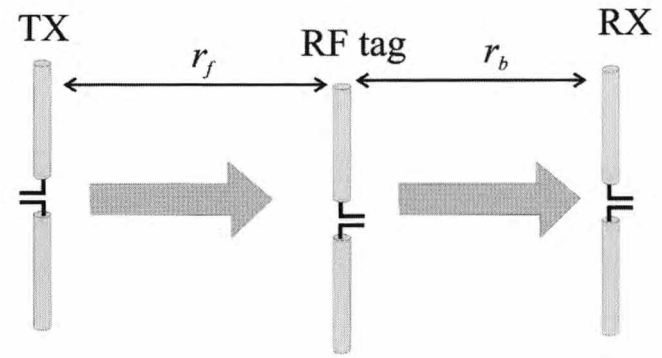

Figure 3c. The bistatic dislocated configuration, one of the three main antenna configurations in the backscatter link.

is the monostatic fade margin. In addition to the familiar loss terms from the power-up link budget, an additional modulation factor, M, must be taken into consideration: this factor is explained in Section 4.1. Note that Equation (2) is just a slight variation of the radar equation, where scattered power falls off as r^4. The monostatic link architecture is often used in commercial RFID readers, although it has the disadvantage of extreme self-interference. Such readers typically rely on a directional coupler or circulator to isolate the powerful, unmodulated transmitted signal from the weak, incoming backscattered signal. Typical circulators can isolate the transmitted carrier from the received signal by 20-30 dB, but reflection of the transmitted signal from the antenna will pass directly through the circulator (or directional coupler), and dominate the incoming backscattered signal by several orders of magnitude [7]. Thus, the range of information exchange for monostatic readers can be limited by their self-interference, rather than by their in-band thermal noise. One way to improve this limitation is to use active cancellation to remove the self-interference signal [8, 9]. However, the ranges of current UHF passive RFID systems are still limited by their power-up threshold, rather than by self-interference or thermal noise. If the power-up efficiency of tag radio-frequency integrated circuits was improved substantially, passive tags would soon become information limited on the backscatter link [10].

3.3 The Bistatic, Collocated Backscatter Link Budget

A second type of backscatter architecture occurs when the reader is bistatic, and the antennas used to transmit and receive are located in the same local area (within a few wavelengths of one another). In this case, the linear-scale link budget for the received modulated backscatter power, P_R, is

$$P_R = \frac{P_T G_T G_R G_t^2 \lambda^4 X^2 M}{(4\pi r)^4 \Theta^2 B^2 F_\alpha}, \tag{3}$$

where F_α is the bistatic, collocated fade margin, G_T is the load-matched, free-space gain of the reader's transmitter antenna, and G_R is the load-matched, free-space gain of the reader's receiver antenna. There are two key differences between Equation (3) and the monostatic link described in Equation (2). First, the reader's transmitter and receiver antennas can have different gains, G_T and G_R, respectively. Second, a different fading factor, F_α, must be used, since the small-scale fading is no longer identical on the reader-to-tag and tag-to-reader links. This difference is discussed in detail in Section 4.6.

3.4 The Bistatic, Dislocated Backscatter-Link Budget

A third and final type of backscatter-link budget describes an RF tag reader where two different antennas at two separate locations are used: one to transmit, and the other to receive. In this case, the received modulated backscattered power, P_R, in a linear scale is given by

$$P_R = \frac{P_T G_R G_T G_t^2 \lambda^4 X_f X_b M}{(4\pi)^4 r_f^2 r_b^2 \Theta^2 B_f B_b F_\beta}, \tag{4}$$

where r_f is the reader-to-tag link separation distance [m], r_b is the tag-to-reader link separation distance [m], X_f is the reader-to-tag link polarization mismatch, X_b is the tag-to-reader link polarization mismatch, B_f is the reader-to-tag link path-blockage loss, B_b is the tag-to-reader link path-blockage loss, and F_β is the bistatic, dislocated small-scale fading loss. Note that many of the loss terms must now account for the two different paths that radio waves take from the transmitter to the RF tag and from the RF tag to the receiver. Also, the average RF tag gain, G_t, is only approximate for Equation (4), since the angles-of-arrival and angles-of-departure are different for waves incident upon and scattered from the RF tag. This difference is caused by the separation between the reader's transmitter and receiver antennas, and the RF tag antenna gain's dependence upon azimuth and elevation angle.

To clarify the notation in Equation (4), it should be understood that the RF channel in which a backscatter-radio system operates is composed of two parts: the forward link and the backscatter link. The forward link, also called the reader-to-tag link, describes signal propagation from the reader's transmitter to the RF tag, and link-budget parameters that pertain to this link are denoted by a subscript *f*. Similarly, the backscatter link, or the tag-to-reader link, describes signal propagation from the RF tag to the reader receiver, and link-budget parameters that pertain to this link are denoted by a subscript *b*. These terms will be used interchangeably throughout this article.

4. Radio-Channel Impairments

This section presents a more-detailed explanation and quantification of the physical propagation mechanisms that affect backscatter-radio propagation.

4.1 Modulation Factor

The amount of reflected power in a backscatter link is not only a function of the antenna properties of the RF tag and its surrounding materials. Since 1s and 0s must be coded with two different reflection states, the power of the digital information scattered toward the reader is also related to the *difference* in load states. If Γ_A is the reflection coefficient at the antenna for state *A*, and Γ_B is the reflection coefficient at the antenna for state *B* (as illustrated in Figure 4), then the amount of reflected power will be proportional to the modulation factor, *M*, given by [11]

$$M = \frac{1}{4}\left|\Gamma_A - \Gamma_B\right|^2, \tag{5}$$

where the reflection coefficient for each state is defined as [18]

$$\Gamma_{A,B} = \frac{Z_{\text{RFIC}}^{A,B} - Z_{\text{ant}}^*}{Z_{\text{RFIC}}^{A,B} + Z_{\text{ant}}}, \tag{6}$$

and $Z_{\text{RFIC}}^{A,B}$ is the input impedance of the RF port of the radio-frequency integrated circuit in states *A* or *B*, Z_{ant} is the input impedance of the antenna, and $(\cdot)^*$ is the complex-conjugate operator. Equation (5) is maximized when ideal open- and short-circuit loads are used to modulate the 1s and 0s, resulting in +1 and −1 reflection coefficients, respectively. These extreme reflection coefficients may be quite difficult to achieve in practice. This becomes most difficult when the RF tag's antenna approaches metallic objects, making it impossible for semiconductor devices to make an RF short circuit *relative* to the plummeting radiation resistance of the near-metal tag antenna. Furthermore, the choice of the modulation factor presents a tradeoff in design parameters [7]. If the reflection coefficients were switched between an open and short circuit, then all power would be backscattered, and the power-up circuitry of the tag's radio-frequency integrated circuit would be starved of available power. Instead, some designers choose to use amplitude-shift-keying (ASK) modulation, and to switch the reflection coefficient between a matched load and a

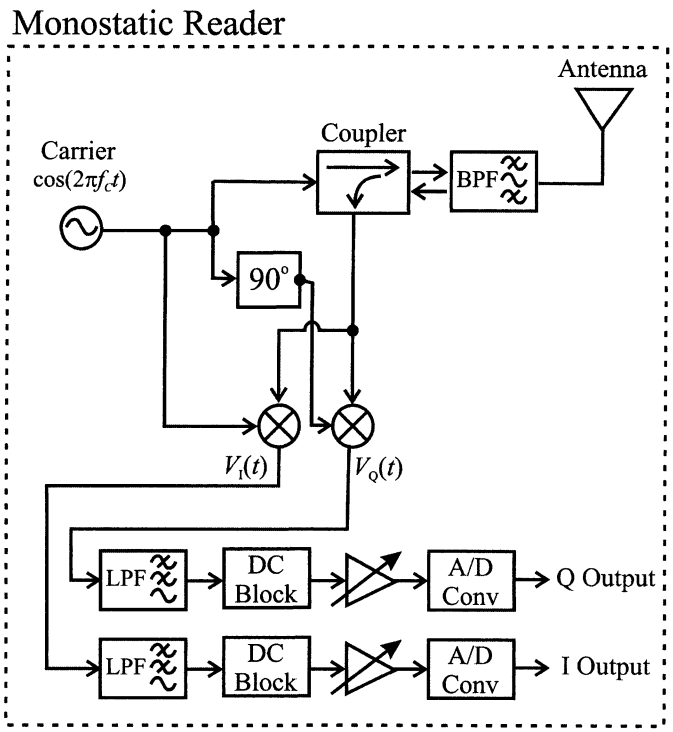

Figure 4a. A block diagram of a monostatic RFID reader system.

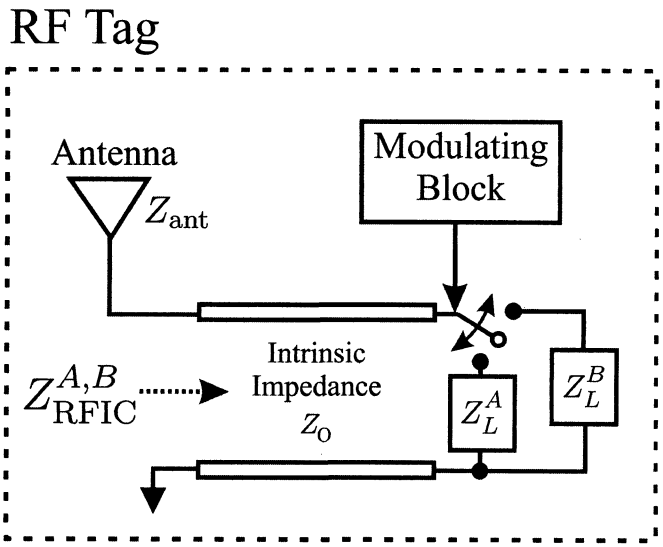

Figure 4b. A block diagram of a single-antenna RF tag.

short, $M = 0.25$, to balance the power backscattered and absorbed by the radio-frequency integrated circuit [6]. Others use phase-shift-keying (PSK), and simply modulate the reactive component of the chip's impedance [5]. This allows constant power to be supplied to the radio-frequency integrated circuit, regardless of the modulation state.

An alternative method for characterizing the power scattered from the RF tag is to use the tag's effective *radar cross section* (RCS). Over the years, much research on the RCS of loaded antennas has been done, with the goal of making "stealthy" antennas – antennas with zero RCS (non-scattering) – for military applications. However, for modulated-backscatter applications the goal is to maximize an antenna's RCS, while still absorbing enough power to turn on the tag's radio-frequency integrated circuit. The theory of loaded-antenna RCS for modulated backscatter applications has been presented by Nikitin and Rao [12], Penttilä et al. [13], and Fuschini et al. [14], among others. For such applications, the RCS, σ_{RCS}, is related to the tag antenna's gain, G_t; the wavelength of radiation, λ; and the reflection coefficient, $\Gamma_{A,B}$:

$$\sigma_{RCS} = \frac{\lambda^2 G_t^2}{4\pi}\left|\Gamma_{A,B}\right|^2, \tag{7}$$

where $\Gamma_{A,B}$ is defined in Equation (6). In this characterization, the RFID tag may be seen as modulating information back to a reader by changing its effective electromagnetic area: the size of its scattering cross section.

It should be noted that the RCS in Equation (7) is actually the "*modulatable*" RCS of a tag antenna. Superimposed atop this cross section there will also be a *structural* RCS of a tag antenna, due to the fact that any conducting object will scatter electromagnetic waves. The full RCS is given by

$$\sigma_{RCS} = \frac{\lambda^2}{4\pi} G_t^2 \left|A_s - \Gamma_{A,B}\right|^2, \tag{8}$$

where A_s is a complex-valued term that represents the structural component [15]. If the difference between modulation states is written in terms of the RCS, the *differential RCS*, $\Delta\sigma_{RCS}$ [16], is

$$\Delta\sigma_{RCS} = \frac{\lambda^2 G_t^2}{4\pi}\left|\Gamma_A - \Gamma_B\right|^2. \tag{9}$$

4.2 On-Object Antenna Gain Penalties

While a tag's antenna may perform well when separated by several wavelengths from conductive and dielectric materials, tag operation may cease completely when it is brought close or attached to an object. Aside from altering the input impedance (discussed in Section 4.5), object attachment reduces the antenna's radiation efficiency and distorts the antenna pattern. This limits both the backscattered power for communication and, for a passive RF tag, the power available for radio-frequency integrated circuit operation. In Equations (1)-(4), the on-object gain penalty, Θ, accounts for these losses. It is defined in a linear scale as the ratio of the load-matched, free-space gain, G_t, of the RF tag's antenna to the gain of the RF tag's antenna attached to an object, $G_{\text{on-object}}$:

$$\Theta = \frac{G_t}{G_{\text{on-object}}}. \tag{10}$$

To make Θ a useful "rule-of-thumb" for design engineers, the power used to calculate G_t and $G_{\text{on-object}}$ in Equation (10) should be averaged over the half-space facing away from the object, so that Θ is independent of the angle-of-arrival of waves at the RF tag. Unfortunately, calculating $G_{\text{on-object}}$ is difficult analytically, and is complicated by the Θ's dependence on material properties, object geometry, frequency, and antenna type. Therefore, the best method to determine $G_{\text{on-object}}$ is through careful simulation or measurement.

Measurements for several representative cases, shown in Table 1, have shown that Θ can range from 0.9 dB on cardboard to 10.4 dB on an aluminum slab [17]. Initially, some of the gain penalties in Table 1 may not seem significant. However, recall that the backscatter link decreases as $1/\Theta^2$, so an aluminum slab may result in over 20 dB of excess loss.

4.3 Path Blockages

Path blockages in conventional wireless links result in serious but surmountable losses in the link budget. In today's passive UHF backscatter systems, path blockages are usually catastrophic to operation. However, there are some instances when a line-of-sight (LOS) radio channel is not necessary, particularly for battery-assisted RF tags. In these cases, we can borrow the standard modeling techniques for path blockages in conventional wireless systems: the log-normal distribution. In this model, the distribution of possible aggregate blockage losses, B (in dB), can be modeled with the following probability density function:

$$f_B(b) = \frac{1}{\sigma_B\sqrt{2\pi}}\exp\left[-\frac{(b-\mu_B)^2}{2\sigma_B^2}\right], \tag{11}$$

where b is the index of the probability density function, μ_B is the average value of the aggregate blockage loss, and σ_B is its standard deviation, all with units of dB.

Typically, one would use the average value, $B = \mu_B$, in the link budget, and add multiples of a standard deviation, σ_B, as a

Table 1. On-object gain penalties for various materials measured at 915 MHz with a dB scale [17].

Cardboard Sheet	Acrylic Slab	Pine Plywood	De-Ionized Water	Ethylene Glycol	Ground Beef	Aluminum Slab
0.9	1.1	4.7	5.8	7.6	10.2	10.4

margin for increased reliability. Note that for monostatic or bistatic collocated antennas, the RF signal will travel in opposite directions through the same pathways, experiencing the same path blockages *twice*. In the bistatic, dislocated configurations, the reader-to-tag and tag-to-reader pathways are no longer identical, and require separate blockage factors: B_f and B_b, respectively.

To date, there are few studies on RF tag "radioscapes" that would suggest valid parameters for this model. Most planners simply ignore blockages, assuming that there will be a line-of-sight from the reader to the RF tag. As ranges improve and new applications are added, this assumption will become invalid.

4.4 Polarization Mismatch

The polarization mismatch, X, between the reader and tag antennas may vary from 0 to 1 in a linear scale. X is the polarization mismatch factor, and accounts for the power lost due to polarization mismatch [18]. It is often difficult to gauge the exact mismatch factor, since the reader and tag may have unpredictable orientations with respect to one another. If orientation in the system is unpredictable, a median value of $X = 0.5$ (in a linear scale) is commonly assumed for the one-way link. In most collocated backscatter links, this loss is *squared*, since the RF signal travels back and forth between the reader and tag antennas.

In bistatic backscatter links, where the transmitting and receiving antennas are differently polarized with respect to the tag, it is no longer sufficient to simply square the polarization-mismatch factor. In this case, reader-to-tag and tag-to-reader mismatch factors – X_f and X_b, respectively – must be calculated separately.

4.5 Power Transmission Coefficient

The RF tag antenna gain reported in the link budgets assumes an ideal conjugate match between the radiation and load impedances. However, many factors may result in a power-reducing mismatch. These mismatching effects may be caused by the alteration of the antenna's radiation impedance by coupling into nearby objects, or radio-frequency integrated circuit loading of the antenna that results in extreme or transient load impedances. Given an antenna impedance, Z_A, and a load impedance, Z_L, the power transmission coefficient, τ [18, 19] – the normalized power delivered to the load – is

$$\tau = \frac{4\mathcal{R}e\{Z_A\}\mathcal{R}e\{Z_L\}}{\mathcal{R}e\{Z_A + Z_L\}^2 + \mathcal{I}m\{Z_A + Z_L\}^2}, \quad 0 \le \tau \le 1. \qquad (12)$$

When $Z_A = Z_L^*$, where $(\cdot)^*$ is the complex-conjugate operator, maximum power transfer occurs, and $\tau = 1$.

4.6 Small-Scale Fading

In a backscatter-radio system, the power received by the RF tag or backscattered to the reader may vary drastically as a function of RF tag position – even when a line-of-sight path exists between the reader and the RF tag. This variation, known as *small-scale fading*, is caused by the constructive and destructive interference of waves scattered from objects in the vicinity of the backscatter-radio system. In a small-scale fading channel, characterization of the received signal is accomplished by modeling the received signal as a random variable the value of which is determined by a prescribed probability distribution. The distribution used is determined by the link budget in question and the propagation characteristics of the channel. Once a probability distribution has been chosen, a safety factor, or *fade margin*, is included in the link budgets to ensure that the backscatter-radio system can operate with a certain outage probability. For any channel, the fade margin in dB can be calculated as

$$\text{Fade Margin} = 10\log_{10}\left\{\frac{\left[F_R^{-1}(\text{Outage Probability})\right]^2}{P_{av}}\right\}, \qquad (13)$$

where F_R is the CDF of the received signal envelope, and P_{av} is the average power in the channel (in units of envelope-squared). The key for this calculation is choosing the appropriate distribution.

4.6.1 The Power-up Fade Margin, F

The two probability distributions most commonly chosen to model fading in the power-up link budget are the Rayleigh and Rician distributions. A Rician distribution is used when a line-of-sight path exists between the reader and the RF tag; otherwise, the Rayleigh distribution is used. The level of fading is described by the Rician K factor: the ratio of the power in the specular line-of-sight signal and the power in the non-specular, scattered signal. Reported Rician K factors for backscatter channels are $-\infty$ dB and 2.8 dB [20], although higher values are certainly possible. These numbers represent the K factors of the individual reader-to-tag and tag-to-reader links, where it has been assumed that each link has the same K factor.

4.6.2 The Monostatic Backscatter Link Fade Margin, F_2

Fading in the monostatic backscatter link, although caused by the same physical mechanisms, has a radically different distribution than that of the power-up link. The reason for this difference is that the fading in the reader-to-tag link is multiplied by the fading in the tag-to-reader link. The fading of the backscattered signal can be modeled using a product-Rayleigh (for the non-line-of-sight (NLOS) case) or a product-Rician (for the line-of-sight case) distribution. Since a single antenna is used to transmit and receive in a monostatic reader, the reader-to-tag and tag-to-reader links are identical. Intuitively, this means that there is a strong relationship (i.e., a high level of correlation) between the fading in the reader-to-tag and tag-to-reader links, which results in the deepest fading of all the backscatter link budgets [21].

4.6.3 The Bistatic Collocated Backscatter Link Fade Margin, F_α

The bistatic collocated link differs from the monostatic link in that two separate – but closely spaced – reader antennas are used to transmit and receive. In terms of fading, this means that the reader-to-tag and tag-to-reader links will be less correlated. Hence, when compared to the monostatic backscatter link, fading in the bistatic collocated link will always be less severe, because the likelihood that both halves of the link will fade simultaneously is less.

4.6.4 The Bistatic Dislocated Backscatter Link Fade Margin, F_β

In the bistatic dislocated backscatter link, the reader transmitter and receiver antennas are separated by a large electrical distance. This large separation causes the fading in the reader-to-tag and tag-to-reader links to be statistically uncorrelated. Therefore, the fading in this link will be the least severe of all the backscatter links, but still worse than the power-up link.

4.6.5 Calculated Fade Margins

Table 2 shows fade margins for several different channels and levels of fading. The left column gives the outage probability, defined as $Pr\left[P_R \le (P_{av}/\text{FadeMargin})\right]$ or, in words, the probability that the received power, P_R, has dropped below the average power, P_{av}, by an amount equal to the fade margin. Therefore, for the power-up link with $K = 0$ dB, Table 2 shows that the required fade margin, F, to guarantee that signal fades render the system inoperable with a only a 10% probability is 9 dB. In other words, an additional 9 dB of power must be transmitted to limit system failures to a 10% frequency. In Table 2, F_2 and F_β represent the two extreme levels of link correlation for the monostatic and bistatic dislocated backscatter link budgets, respectively. Although not included in the table, the fade margin for the bistatic, collocated link budget, F_α, will be in the range $F_2 < F_\alpha < F_\beta$.

5. Illustrative Examples

5.1 An RFID Portal at 915 MHz

In this section, we will demonstrate the link budgets described in Section 3 through an example of an RFID portal operating at 915 MHz. We proceed by defining the RF tag system parameters, describing the propagation environment, and then plotting the link budgets as a function of the reader-to-tag separation distance for two different object attachments.

5.1.1 RF Tag Reader

In this system, tagged objects pass through a passageway, or portal, to which the reader's antennas are fixed. The reader has the ability to operate with a single transmitter and receiver antenna (monostatic mode), or with two widely-spaced transmitter and receiver antennas (the dislocated bistatic mode). In either mode, the transmitter and receiver antennas are right-hand-circularly polarized patch antennas, which resonate at 915 MHz with a gain of 7 dBi. The sensitivity of the reader is −80 dBm [10,22].

5.1.2 RF Tag

Figure 5 shows the equivalent circuit of the RF tag antenna, the impedance-transformation network, and the antenna port of the tag's radio-frequency integrated circuit. The RF tag uses a single folded-dipole antenna, which is linearly polarized with a free-space, load-matched gain of 2.1 dBi and an approximate free-space terminal impedance of $300 + j100\,\Omega$, determined from Figure 6b [11]. The input impedance at the antenna port of most tag radio-frequency integrated circuits can be modeled as a series resistor of a few ohms (often less than 30 Ω), in series with a capacitor that is a fraction of a picofarad [7]. For this example, we will assume that the tag's radio-frequency integrated circuit uses ASK modulation and switches its impedance between two states, $Z^A_{\text{RFIC}} = 20 - j350\,\Omega$ and $Z^B_{\text{RFIC}} = 2 - j0.1\,\Omega$ (an approximate short circuit). The nonzero input impedance of Z^B_{RFIC} reflects the fact that field-effect transistors cannot provide a true short circuit, but are modeled as a small shunt resistance in parallel with a small capacitance, the values of which depend upon the transistor's

Table 2. Small-scale fade margins for one-way (F), monostatic (F_2), and bistatic dislocated (F_β) backscatter links. The fade margins are reported in dB.

	$K = -\infty$ dB			0 dB			$K = 3$ dB			$K = 10$ dB		
Outage Probability	F	F_2	F_β	F	F_2	F_β	F	F_2	F_β	F	F_2	F_β
0.5	2	6	4	1	5	3	1	3	2	0	1	1
0.1	10	22	15	9	20	14	7	16	11	3	7	5
0.05	13	29	19	12	26	17	10	21	15	4	9	6
0.01	20	43	28	19	40	26	16	34	22	6	13	9
0.005	23	49	32	22	46	29	19	40	26	7	15	10
0.001	30	63	40	29	60	37	26	54	33	9	20	13

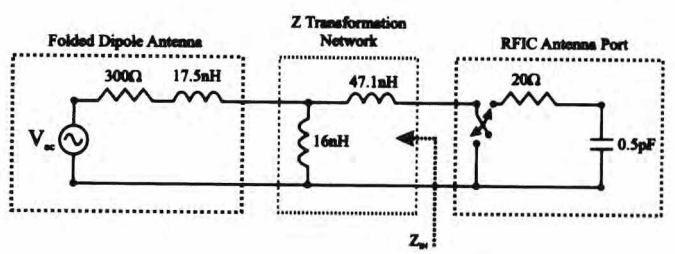

Figure 5. The equivalent circuit of the folded-dipole RF tag antenna, impedance-transformation network, and radio-frequency integrated circuit antenna port used in the 915 MHz portal example.

implementation and biasing. For efficient power transfer from the antenna to the tag's radio-frequency integrated circuit, a matching network is used to transform the antenna impedance to $Z_{IN} = 20 + j350\,\Omega$, creating a conjugate impedance match with the tag's radio-frequency integrated circuit in impedance state *A*. In most RF tags, lumped-element impedance-transformation networks are not used; instead, the necessary inductance or capacitance is incorporated directly in the structure of the planar antenna [7]. In this example, the matching network is treated separately from the antenna structure for illustrative purposes. As mentioned previously, the power required for the tag to power up varies widely by design. In this example, we assume that -13 dBm is required at 915 MHz [4, 10].

5.1.3 The Propagation Environment

The RF tag system operates in a cluttered environment that experiences small-scale fading due to multipath propagation. As the RF tag passes in front of the reader's antennas, a line-of-sight path exists, resulting in a Rician *K* factor of 3 dB. Furthermore, it is assumed that no blockages impair the line-of-sight path. For illustration of one of the worst-case propagation scenarios, we assume that the tagged objects passing through the portal are made of aluminum, and that a 5% outage probability is desired.

5.1.4 Link-Budget Calculations

The information in the previous paragraphs, combined with Table 1 and Table 2, provide all of the parameters necessary to calculate the terms in the link budgets. A brief description of each is provided below, and summarized in Table 3.

5.1.4.1 Transmitted Power, P_T

In the United States, the Federal Communications Commission (FCC) limits the power that an RF tag system can transmit to 4 W of equivalent isotropic radiated power (EIRP). EIRP power is simply the product of the transmitted power and the transmitter-antenna gain ($P_{EIRP} = G_T P_T$) with a linear scale. Since the reader's antennas have a gain of 7 dBi (5 in a linear scale), the maximum continuous-wave (CW) power transmitted is limited to 29 dBm (or 800 mW).

5.1.4.2 Modulation Factor, M, and Power Transmission Coefficient, τ

The RF tag modulates backscatter by switching its input impedance between two states. When the RF tag is attached to a cardboard object, the antenna's impedance changes little from its free space value, $Z_{IN} = 20 + j350\,\Omega$, as seen at the output of the impedance-transformation network. Using Z_{IN}, Z^A_{RFIC}, and Z^B_{RFIC} in Equation (5), the modulation factor on cardboard is found to be $M = 0.25$. Using Equation (12), the power transmission coefficient on cardboard is $\tau = 1$.

As the RF tag is brought close to an aluminum object, the impedance of the folded-dipole antenna drops rapidly, as shown in Figure 6a. For a very small object-to-tag separation distance of 0.005λ – which approximates object attachment – the terminal impedance of the antenna drops to approximately $0.5 + j25\,\Omega$. The corresponding impedance, seen at the output terminals of the impedance-transformation network, is $Z_{IN} = 0.31 + j290\,\Omega$. This assumes that the values of the impedance-transformation network are not altered by close metal proximity: an assumption that may not be valid for a matching network incorporated into the antenna structure. Using Z_{IN}, Z^A_{RFIC}, and Z^B_{RFIC} in Equation (5) and Equation (12), the modulation factor and power transmission coefficient are found to be $M = 3.5\times10^{-5}$ and $\tau = 6.2\times10^{-3}$, respectively (both in a linear scale).

5.1.4.3 Gain Penalty, Θ

From Table 1, the gain penalties for cardboard and metal are $\Theta = 0.9$ dB (1.2 in a linear scale) and $\Theta = 10.4$ dB (11 in a linear scale), respectively.

5.1.4.4 Fade Margins

To maintain a 5% outage probability in a multipath environment with $K = 3$ dB, the required fade margins from Table 2 are $F = 10$ dB (10 in a linear scale) for the power-up link, $F_2 = 21$ dB (126 in a linear scale) for the reader in the monostatic mode, and

Table 3. 915 MHz RF tag portal example parameters in a linear scale.

Material	P_T [mW]	$G_{T,R}$	G_t	$X_{f,b}$	F	F_2	F_β	λ [m]	M	τ	Θ	B
Cardboard	800	5	1.6	0.5	10	126	32	0.33	0.25	1	1.2	1
Aluminum	800	5	1.6	0.5	10	126	32	0.33	3.5×10^{-5}	6.2×10^{-3}	11	1

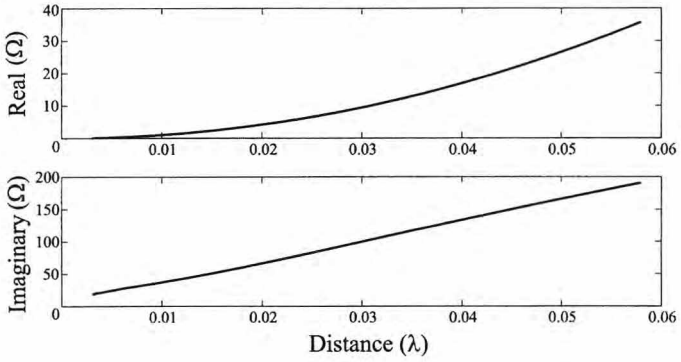

Figure 6a. The folded-dipole antenna's impedance (simulated using the *Numerical Electromagnetics Code* (*NEC*), a Method-of-Moments-based code), as a function of the electrical distance from a perfectly conducting half-plane at 915 MHz [11] for electrical spacings of 0.005λ to 0.06λ.

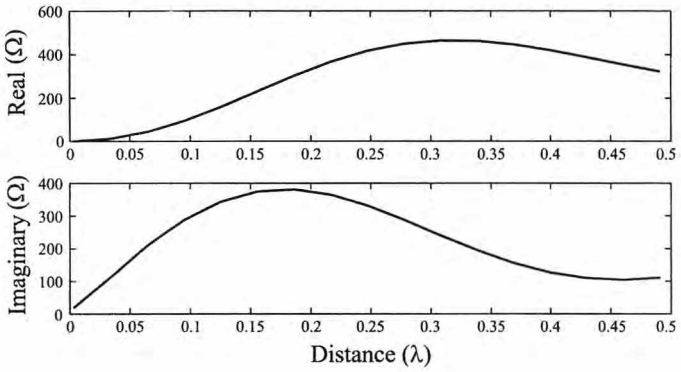

Figure 6b. The folded-dipole antenna's impedance (simulated using the *Numerical Electromagnetics Code* (*NEC*), a Method-of-Moments-based code) as a function of the electrical distance from a perfectly conducting half-plane at 915 MHz [11] for electrical spacing of 0.005λ to 0.5λ

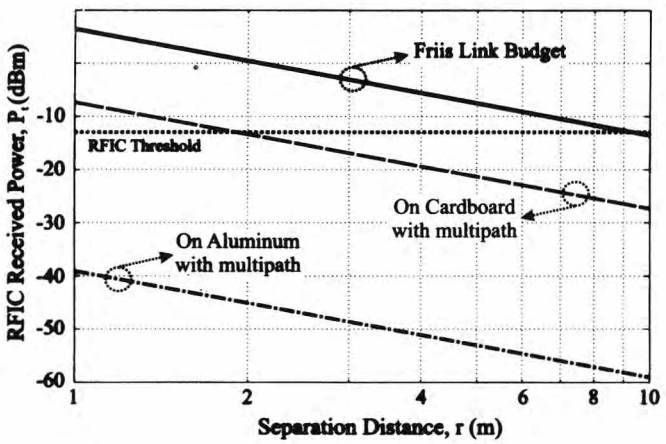

Figure 7a. The power-up link plotted as a function of reader-to-tag separation distance, *r*.

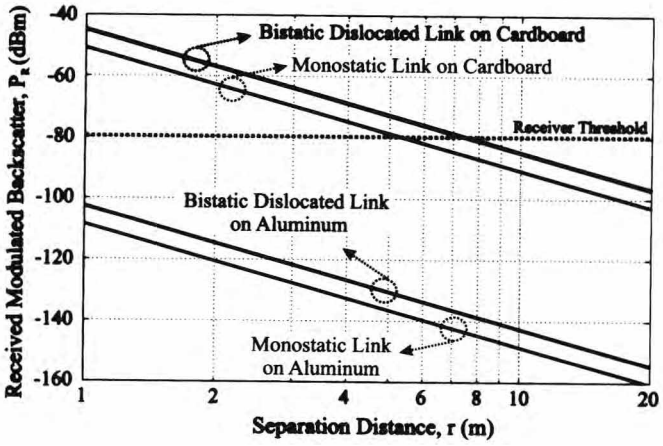

Figure 7b. The backscatter link plotted as a function of reader-to-tag separation distance, *r*.

$F_\beta = 15$ dB (32 in a linear scale) for the reader in the bistatic dislocated mode.

5.1.4.5 Polarization Mismatch, X

Since the reader's antennas are circularly polarized and the RF tag antenna is linearly polarized, a 3 dB polarization mismatch will result on both the reader-to-tag and tag-to-reader links. Therefore, $X_f = X_b = 0.5$ in a linear scale.

5.1.5 Discussion

Figure 7a shows plots of the power-up link, described by Equation (1), for three different cases. In the first power-up link budget, X, τ, Θ, B, and F are all equal to one (in a linear scale). This is the Friis free-space link budget: a link budget that assumes free-space path loss, no impedance or polarization mismatches, no path blockages, and no multipath fading. The second case is the power-up link for an RF tag attached to cardboard, and the third is the power-up link for an RF tag attached to an aluminum object. Note the extreme optimism of the Friis free-space link budget. Compared to the realistic second and third cases, an RF tag system designed using the Friis link budget may overestimate its range by several meters. In the second case, although cardboard attachment itself does little to affect the tag's operation, fading and polarization mismatches reduce the range of the RF tag to less than 2 m. In the third case, the reduced antenna impedance results in an extremely small power transmission coefficient, τ, that prevents the RF tag from turning on.

Similarly, Figure 7b shows plots of the backscatter links described by Equation (2) and Equation (4) for an RF tag attached to cardboard and aluminum. A brief comparison of Figure 7a and Figure 7b shows that the range of the RF tag is limited by the power-up link, not by the backscattered power. The effect of the reader's antenna configuration is also seen: the monostatic link is several dB worse than the bistatic, dislocated case, regardless of material attachment. Like the power-up link, the low antenna impedance caused by aluminum attachment results in an extremely small modulation factor, M. The small amount of modulated power scattered from the RF tag is below the reader's sensitivity threshold and therefore is undetected.

5.2 The Advantages of High-Frequency Backscatter Systems

As evident in Section 5.1, even a small change in the parameters of the link budgets can have a significant effect on the range of an RF tag. Therefore, any method to increase antenna gain, minimize material effects, and/or reduce fading is welcome news to the backscatter-tag designer. One way to make such improvements possible is by operating backscatter RF tags at a higher frequency. In the US, the two most commonly used RF-tag frequency bands are the 902-928 MHz industrial, scientific, and medical (ISM) band, and the 2400-2483.5 MHz ISM band; however, another ISM band is available at 5725-5850 MHz. In this band, the wavelength is much smaller than that found in the 902-928 MHz band, and leads to the following improvements.

First, antennas in the 5725-5850 MHz ISM band can be made small enough for multiple antennas to be used on each RF tag, without increasing – and possibly decreasing – the tag's footprint size compared to the footprint of a 902-928 MHz RF tag. This is because antennas scale with wavelength, shown graphically in Figure 8. Using multiple RF tag antennas will reduce the fade margins required for backscatter-radio-system operation – especially in non-line-of-sight channels [23]. Mi [24] has shown that multiple, closely-spaced antennas can be used to increase the power received by an RF tag. Multiple RF tag antennas may also allow diversity schemes to be employed in the RF tag, to mitigate fading in its received power [25]. In addition, fade mitigation and direction finding will be aided by the very compact antenna arrays that are available for readers in the 5725-5850 MHz band. Such arrays will even be small enough for use on mobile and hand-held readers.

Second, higher reader and tag antenna gains are possible in the 5725-5850 MHz band. For a fixed antenna aperture, Equation (14) dictates that the gain of the RF tag antenna will increase with frequency [18]:

$$G = \frac{4\pi}{\lambda^2} A_{\text{eff}}, \qquad (14)$$

where G is the antenna's gain in a linear scale, λ is the wavelength [m], and A_{eff} is the effective area of the antenna [m^2].

Third, operating in the 5725-5850 MHz band will improve an RF tag's on-object performance compared to lower frequencies by increasing the electrical separation between the tag and object. For example, Figure 6a shows that the real impedance at an electrical object-to-tag distance of 0.01λ is $\approx 2\,\Omega$ at 915 MHz. If the physical separation distance is unchanged and the frequency is increased to 5790 MHz, the electrical object-to-tag distance becomes 0.06λ, with a corresponding real impedance of $\approx 40\,\Omega$, resulting in a larger power transmission coefficient, τ, and modulation factor, M.

Fourth, more bandwidth is available in the 5725-5850 MHz ISM band than in the other two ISM bands used for RF tags. This additional bandwidth will enable high-data-rate and spread-spectrum backscatter communication [26].

As an example of gains available at higher frequencies, consider the same RF tag system described in Section 5.1. If this system were redesigned to operate at 5.79 GHz, then the high-frequency benefits described above would apply. The resulting changes in the link-budget parameters are described in the following paragraphs, and summarized in Table 4.

5.2.1 Increased Antenna Gain

If the antenna's effective area remains constant, Equation (14) dictates that an additional 16.4 dB of gain is available as λ decreases from 33 cm at 915 MHz to 5 cm at 5.79 GHz. Therefore, at 5.79 GHz, the reader's antenna gains are now 23.4 dBi

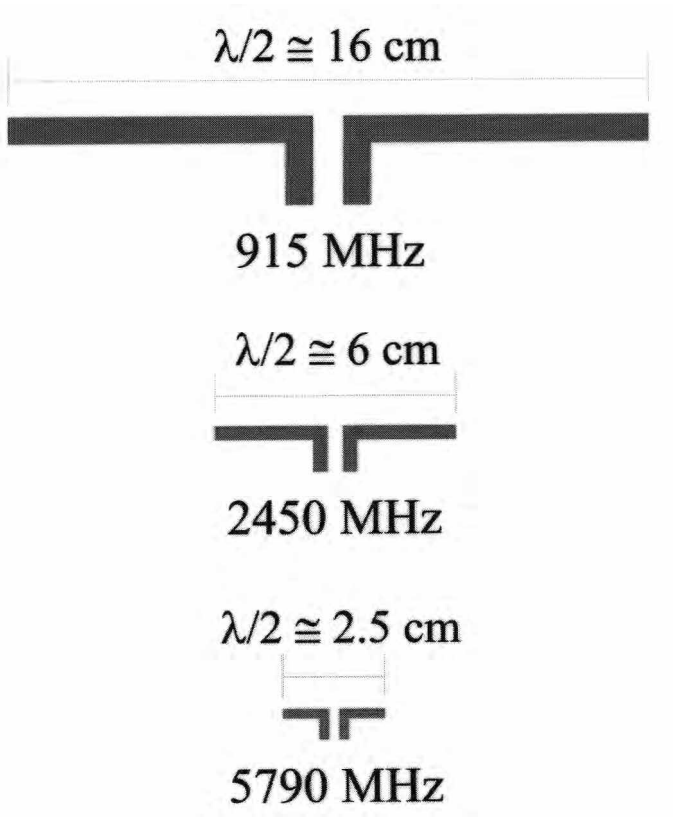

Figure 8. Half-wave dipoles for 915 MHz, 2450 MHz, and 5790 MHz, drawn proportionally (not actual size) to show the relative decrease in size with increasing frequency.

Table 4. 5.79 GHz RF tag portal example parameters in a linear scale.

Material	P_T [mW]	$G_{T,R}$	G_t	$X_{f,b}$	F	F_β	λ [m]	M	τ	Θ	B
Cardboard	18.3	219	71	0.5	10	6.3	0.05	0.25	1	1.2	1
Aluminum	18.3	219	71	0.5	10	6.3	0.05	4.4×10^{-3}	0.13	11	1

(219 in a linear scale), and the RF tag's antenna gain is now 18.5 dBi (71 in a linear scale).

5.2.2 Multiple Tag Antennas and Maximal Ratio Combining

At 5.79 GHz, it is practical to use two antennas on each RF tag and a two-element antenna array at the reader receiver. If maximal ratio combining (MRC) is performed on the diversity branches received from the two-element receiver array, then F_β is reduced to 8 dB (6.3 in a linear scale) for a 5% outage probability (this result was obtained through Monte Carlo simulation of the backscatter channel). For this example, the power-up fade margin, F, remains unchanged from the 915 MHz example.

5.2.3 Increased Object Immunity

From the example in Section 5.1, the RF tag's antenna attached to a metal object is 0.005λ from the metal surface at 915 MHz. If the RF tag now operates at 5.79 GHz and its physical distance from the metal surface is unchanged, the electrical separation distance becomes 0.033λ. At this distance, Figure 6a shows that the antenna's terminal impedance is now approximately $10 + j100\,\Omega$, which corresponds to $Z_{IN} = 2.3 + j319\,\Omega$ at the output terminals of the impedance-transformation network. From Equation (12) and Equation (5), the power transmission coefficient and modulation factor for metal attachment are now $\tau = 0.13$ and $M = 4.4\times10^{-3}$ (both in a linear scale), respectively. Because of cardboard's weak effect on the antenna's impedance, τ and M for cardboard attachment do not change from the 915 MHz example.

To complete this example, the transmitted power must be decreased to 12.6 dBm (or 18.3 mW) to meet FCC power limitations with the increased reader-antenna gains. Since no measurements of gain penalties at 5790 MHz are available, 915 MHz gain-penalty values from Table 1 are used.

5.2.4 Discussion

Figure 9a compares the power-up link budgets at 915 MHz and 5790 MHz, and shows surprising results. For cardboard attachment, the links are almost identical: the power sacrificed to higher path loss at 5790 MHz is balanced by increased antenna gain at the RF tag. For metal attachment, increased object immunity combines with the increased antenna gain at 5790 MHz to make the link approximately 13 dB better than that at 915 MHz. Similar improvement is seen for the bistatic, dislocated links shown in Figure 9b. Here, the reduced fading, increased RF tag antenna gain, and the greatly increased reader-receiver antenna gain cause the links at 5790 MHz to perform approximately 24 dB and 45 dB better than those at 915 MHz for cardboard and aluminum attachment, respectively.

While these gains still do not now allow the RF tag to operate while attached to the aluminum slab, they may do so for other, less-extreme material attachments, and may result in significant range and reliability improvements. Active tags will immediately benefit from the gains evident in Figure 9b, since their performance is not constrained by the more-stringent power-up link. Passive tags will also experience significant benefits; however, the benefits shown in Figure 9a will be limited in some commonly used tag radio-frequency integrated circuit technologies by parasitic capacitance that increases power consumption at high frequencies. However, with careful circuit layout and use of technologies other than conventional silicon, it should be possible to adequately reduce the power consumption of high-frequency tag radio-frequency integrated circuits at reasonable manufacturing costs. Such high-frequency, low-power radio-frequency integrated circuits will have operating ranges comparable to their low-frequency counterparts, but with the added advantage of reduced fading and increased object immunity. An example of a high-frequency tag radio-frequency integrated circuit with low power consumption, as noted in Section 2, was reported by Curty et al. [6] to consume 2.7 μW (−25 dBm) at 2.45 GHz. This radio-frequency integrated circuit was fabricated using a 0.5 μm silicon-on-sapphire technology.

It should be noted that while the RF tag's antenna gain at 5790 MHz will increase the RF tag's range, it will also increase its directivity. The result will be an RF tag that is more orientation sensitive than that at 915 MHz. If the RF tag's orientation is fixed or its range very small, the increased directivity will not be an

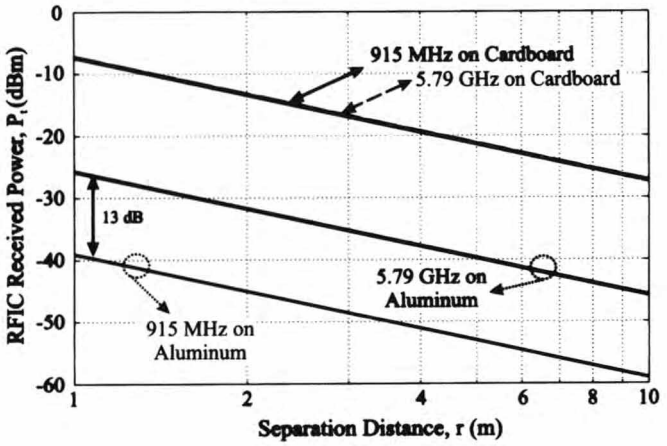

Figure 9a. The power-up link plotted as a function of reader-to-tag separation distance, *r*.

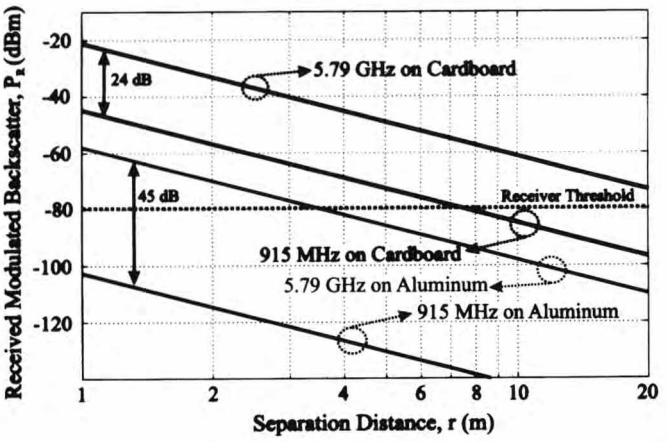

Figure 9b. The backscatter link plotted as a function of reader-to-tag separation distance, *r*.

issue; however, for other applications, it may pose a serious but not insurmountable problem. In such cases, multiple reader antennas can be used to power the RF tag from different spatial positions. Furthermore, as tag radio-frequency integrated circuit technology advances and the required turn-on power is decreased, the RF tag's antenna gain and, as a result, directivity can be reduced without sacrificing tag range.

5.3 Polarization and Antenna Diversity

There is an interesting analogy between backscatter radio polarization and a famous physics problem in optics: one that many students perform in their physics classrooms. In this problem, a light source illuminates a pair of polarizers. If the polarizers are aligned, most of the light passes through. However, if one of the polarizers is tilted 90°, the last polarizer becomes completely dark. Surprisingly, when a third polarizer is inserted at a 45° angle between the two 90° offset polarizers, light passes through all three, albeit attenuated by a factor of four in power (6 dB), as illustrated in Figure 10.

There is a powerful analogy between the optical-polarizer experiment described above and the backscatter link of an RF tag system. Consider the case in the upper portion of Figure 10, where cross-polarized reader antennas are used to read an RF tag. In this case, the RF tag's antenna polarization is aligned with the vertically-polarized transmitter antenna and, therefore, most of the transmitted power will be coupled into the RF tag's antenna. On the other hand, no power will couple into the receiver antenna, because it is cross-polarized to the power that the tag scatters. A solution to this problem is to orient the RF tag's antenna at 45° with respect to the polarization of both reader antennas. Now, a significant portion of the power will be coupled into the RF tag's antenna *and* read by the reader's receiver. An added benefit provided by this setup is an improvement in the system's carrier-to-interference ratio, as there is now significant cross-polarized discrimination between the reader's transmitting and receiving antennas. In fact, based on the polarization properties of the 45° RF tag's antenna in Figure 10, one can imagine a peculiar form of antenna diversity where two linearly-polarized antennas are held at 45° with respect to one another – in contrast to the usual 90° case of polarization-diversity antennas in a conventional wireless link. When interrogated with cross-polarized reader antennas, there is always a spatial orientation in which one of these antennas is capable of both powering-up and scattering information back to the reader [26]. Referring to the illustration in Figure 11, we can see that the polarization mismatches for the RF tag antennas are

$$X_{t1} = X_f X_b = \cos^2(\theta)\underbrace{\cos^2\left(\frac{\pi}{2}-\theta\right)}_{\sin^2(\theta)},$$
$$X_{t2} = X_f X_b = \cos^2\left(\frac{\pi}{4}+\theta\right)\cos^2\left(\frac{\pi}{4}-\theta\right), \quad (15)$$

where X_{t1} and X_{t2} are the total power polarization mismatches on the forward and backscatter links, and θ is the orientation angle with respect to the transmitter. Interestingly, the *sum* of the two polarization mismatch terms in Equation (15) is independent of θ. Circularly-polarized reader antennas are often used for mitigation of polarization-mismatch effects in current RFID systems, but they

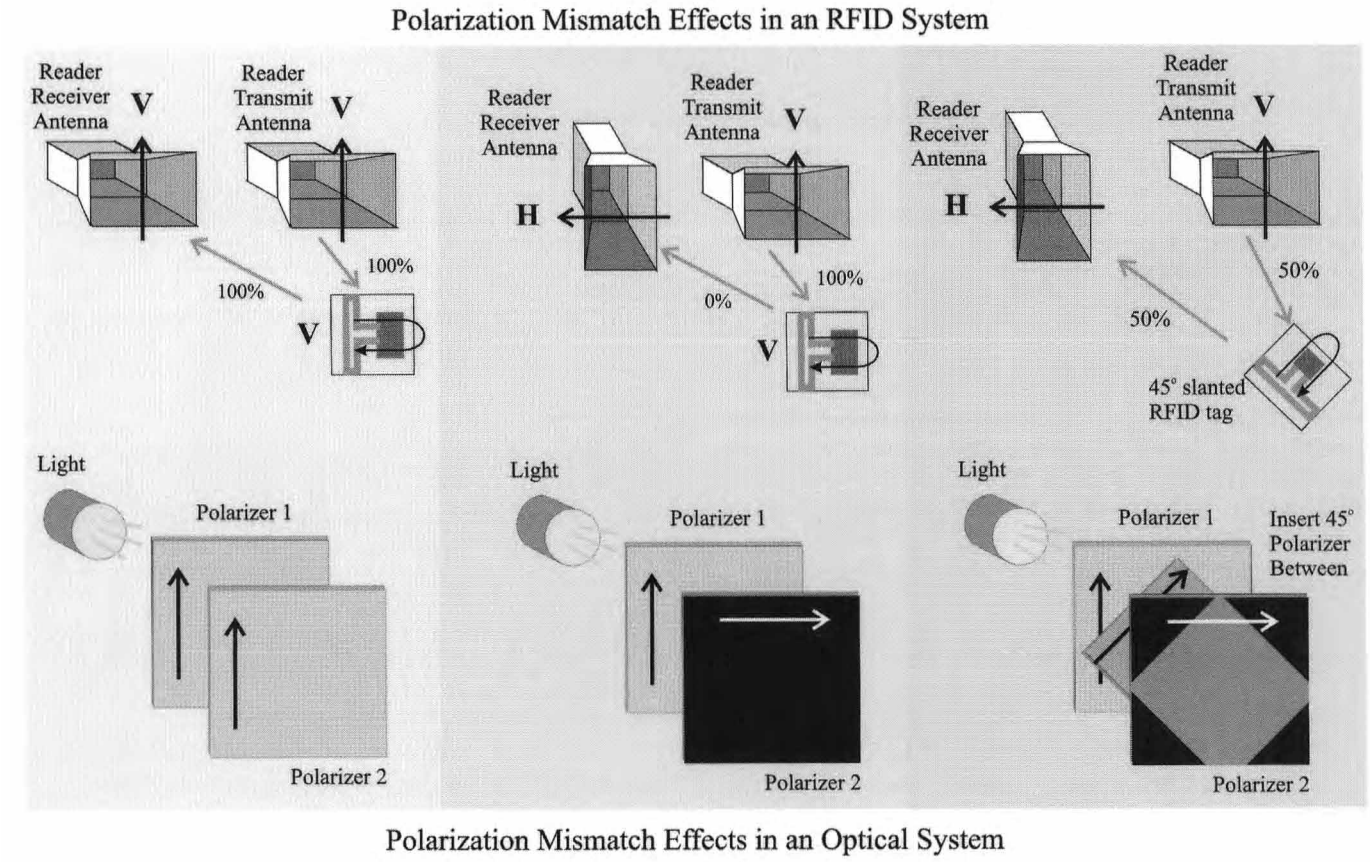

Figure 10. Examples of polarization effects in an RFID link and an analogous optical link.

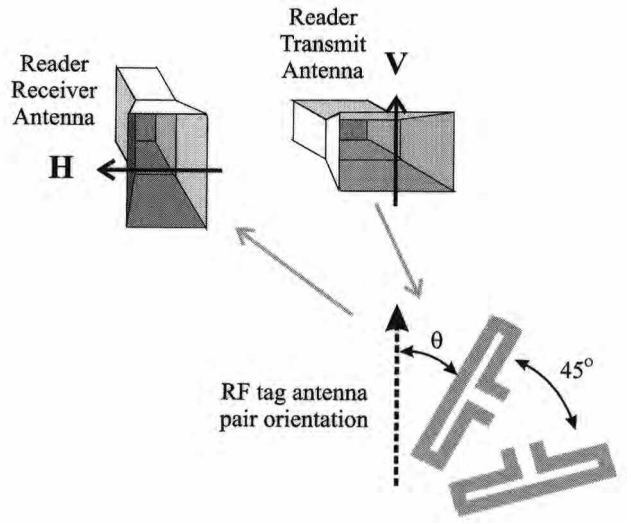

Figure 11. The use of 45°-slant-diversity antennas in a backscatter system with a cross-polarized reader transmitter and receiver.

lack the ability to reduce self-interference, like the bistatic system of Figure 11.

6. Conclusion

Successful backscatter radio design requires more than just accurate link-budget equations: it requires an understanding of the propagation mechanisms that affect both the power available to the RF tag and backscattered to the reader receiver. This article has provided link budgets that describe these powers, along with a detailed description of the modulation factor, on-object gain penalties, path-blockage losses, polarization-mismatch losses, impedance-mismatch losses, and small-scale fading losses. A realistic 915 MHz backscatter-radio example was presented to demonstrate use of the link budgets. It showed that object attachment and multipath fading can significantly impact RF tag range. Furthermore, using multiple, 45° slant antennas on the RF tag, in conjunction with cross-polarized reader transmitter and receiver antennas, will improve backscatter communication by reducing the reader's self-interference. It has also been shown that using multiple RF tag antennas along with compact reader antenna arrays in the 5725-5850 MHz frequency band will provide additional propagation benefits – increased antenna gain, reduced small-scale fading, and increased object immunity – over current, lower-frequency systems. Although some obstacles must be overcome, such high-frequency systems may provide reliable communication to future, compact backscatter RF tags.

7. Acknowledgements

This material is based upon work supported in part by National Science Foundation (NSF) CAREER Grant No. 0546955 and the Center on Materials and Devices for Information Technology Research (CMDITR), an NSF Science and Technology Center (STC), under NSF Grant No. 0120967.

8. References

1. J. D. Griffin, G. D. Durgin, A. Haldi, and B. Kippelen, "How to Construct a Test Bed for RFID Antenna Measurements," IEEE International Symposium on Antennas and Propagation, Albuquerque, New Mexico, 2006.

2. J. F. Dickson, "On-Chip High-Voltage Generation in MNOS Integrated Circuits using an Improved Voltage Multiplier Technique," *IEEE Journal of Solid-State Circuits*, **11**, 3, 1976, pp. 374-378.

3. G. De Vita and G. Iannaccone, "Design Criteria for the RF Section of UHF and Microwave Passive RFID Transponders," *IEEE Transactions on Microwave Theory and Techniques*, **MTT-53**, 9, 2005, pp. 2978-2990.

4. D. M. Dobkin and S. M. Weigand, "UHF RFID and Tag Antenna Scattering, Part I: Experimental Results," *Microwave Journal, Euro-Global Edition*, **49**, 5, 2006, pp. 170-190.

5. U. Karthaus and M. Fischer, "Fully Integrated Passive UHF RFID Transponder IC with 16.7-μW Minimum RF Input Power," *IEEE Journal of Solid-State Circuits*, **38**, 10, 2003, pp. 1602-1608.

6. J. P. Curty, N. Joehl, C. Dehollain, and M. J. Declercq, "Remotely Powered Addressable UHF RFID Integrated System," *IEEE Journal of Solid-State Circuits*, **40**, 11, 2005, pp. 2193-2202.

7. D. M. Dobkin, *The RF in RFID: Passive UHF RFID in Practice*, Burlington, MA, Newnes, 2008.

8. A. Safarian, A. Shameli, A. Rofougaran, M. Rofougaran, and F. De Flaviis, "An Integrated RFID Reader," Proceedings of the IEEE International Solid-State Circuits Conference, San Francisco, CA, 2007, pp. 218-219, 598.

9. J. Lee, J. Choi, K. H. Lee, B. Kim, M. Jeong, Y. Cho, H. Yoo, K. Yang, S. Kim, S.-M. Moon, J.-Y. Lee, S. Park, W. Kong, J. Kim, T.-J. Lee, B.-E. Kim, and B.-K. Ko, "A UHF Mobile RFID Reader IC with Self-Leakage Canceller," Proceedings of the IEEE Radio Frequency Integrated Circuits (RFIC) Symposium, 2007, pp. 273-276.

10. P. Nikitin and K. V. S. Rao, "Performance Limitations of Passive UHF RFID Systems," IEEE International Symposium on Antennas and Propagation *Digest*, Albuquerque, New Mexico, 2006, pp. 1011-1014.

11. J. T. Prothro and G. D. Durgin, "Improved Performance of a Radio Frequency Identification Tag Antenna on a Metal Ground Plane," Master's thesis, Georgia Institute of Technology, 2007; available at http://www.propagation.gatech.edu/Archive/PG_TR_070515_JTP/PG_TR_070515_JTP.pdf

12. P. V. Nikitin and K. V. S. Rao, "Theory and Measurement of Backscattering from RFID Tags," *IEEE Antennas and Propagation Magazine*, **48**, 6, 2006, pp. 212-218.

13. K. Penttilä, M. Keskilammi, L. Sydänheimo, and M. Kivikoski, "Radar Cross-Section Analysis for Passive RFID Systems," *IEE Proceedings on Microwaves, Antennas and Propagation*, **153**, 1, 2006, pp. 103-109.

14. F. Fuschini, C. Piersanti, F. Paolazzi, and G. Falciasecca, "Analytical Approach to the Backscattering from UHF RFID Transponder," *IEEE Antennas and Wireless Propagation Letters*, **7**, 2008, pp. 33-35.

15. R. B. Green, *The General Theory of Antenna Scattering*, PhD dissertation, Ohio State University, 1963.

16. P. V. Nikitin, K. V. S. Rao, and R. D. Martinez, "Differential RCS of RFID Tag," *Electronics Letters*, **43**, 8, 2007, pp. 431-432.

17. J. D. Griffin, G. D. Durgin, A. Haldi, and B. Kippelen, "RF Tag Antenna Performance on Various Materials Using Radio Link Budgets," *IEEE Antennas and Wireless Propagation Letters*, **5**, 2006, pp. 247-250.

18. W. L. Stutzman and G. A. Thiele, *Antenna Theory and Design, Second Edition*, Hoboken, NJ, John Wiley and Sons, 1998.

19. K. V. S. Rao, P. V. Nikitin, and S. F. Lam, "Antenna Design for UHF RFID Tags: A Review and a Practical Application," *IEEE Transactions on Antennas and Propagation*, **AP-53**, 12, 2005, pp. 3870-3876.

20. D. Kim, M. A. Ingram, and W. W. Smith, Jr., "Measurements of Small-scale Fading and Path Loss for Long Range RF Tags," *IEEE Transactions on Antennas and Propagation*, **AP-51**, 8, 2003, pp. 1740-1749.

21. J. D. Griffin and G. D. Durgin, "Link Envelope Correlation in the Backscatter Channel," *IEEE Communications Letters*, **11**, 9, September 2007, pp. 735-737.

22. S. Chiu, I. Kipnis, M. Loyer, J. Rapp, D. Westberg, J. Johansson, and P. Johansson, "A 900 MHz UHF RFID Reader Transceiver IC," *IEEE Journal of Solid-State Circuits*, **42**, 12, 2007, pp. 2822-2833.

23. J. D. Griffin and G. D. Durgin, "Gains for RF Tags Using Multiple Antennas," *IEEE Transactions on Antennas and Propagation*, **AP-56**, 2, 2008, pp. 563-570.

24. M. Mi, M. H. Mickle, C. Capelli, and H. Swift, "RF Energy Harvesting with Multiple Antennas in the Same Space," *IEEE Antennas and Propagation Magazine*, **47**, 5, 2005, pp. 100-106.

25. P. Nikitin and K. V. S. Rao, "Performance of RFID Tags with Multiple RF Ports," IEEE International Symposium on Antennas and Propagation *Digest*, Honolulu, HI, 2007, pp. 5459-5462.

26. A. Rohatgi and G. D. Durgin, "Implementation of an Anti-Collision Differential-Offset Spread Spectrum RFID System," IEEE International Symposium on Antennas and Propagation *Digest*, 2006, pp. 3501-3504.

Introducing the Feature Article Authors

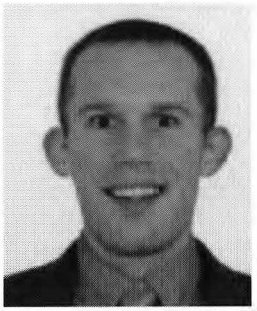

Joshua D. Griffin is a PhD student in Electrical and Computer Engineering at the Georgia Institute of Technology. He completed a BS in Engineering from LeTourneau University in 2003, and an MS in Electrical and Computer Engineering from the Georgia Institute of Technology in 2005. In 2004, Joshua joined the Propagation Group at Georgia Tech, where he researches radio-wave propagation and backscatter-radio applications. In 2006, he participated in a three-month research exchange program with the Sampei Laboratory at Osaka University in Osaka, Japan.

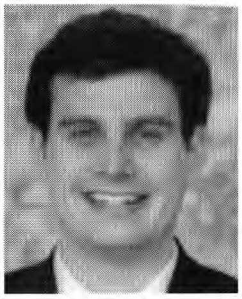

Gregory D. Durgin joined the faculty of Georgia Tech's School of Electrical and Computer Engineering in the fall of 2003. He received the BSEE (1996), MSEE (1998), and PhD (2000) degrees from Virginia Polytechnic Institute and State University. In 2001, he was awarded the Japanese Society for the Promotion of Science (JSPS) Post-Doctoral Fellowship, and spent one year as a visiting researcher with Morinaga Laboratory at Osaka University. In 1998, he received the Stephen O. Rice prize (with coauthors Theodore S. Rappaport and Hao Xu) for best original journal article in the *IEEE Transactions on Communications*. Prof. Durgin also authored *Space-Time Wireless Channels*, the first textbook in the field of space-time channel modeling. Prof. Durgin founded the Propagation Group (http://www.propagation.gatech.edu) at Georgia Tech, a research group that studies radiolocation, channel sounding, direction finding, backscatter radio, RFID, and applied electromagnetics. He is a winner of the NSF Career award as well as numerous teaching awards, including the Class of 1940 Howard Ector Outstanding Classroom Teacher Award (2007). He is an active consultant to industry.